frontiers in Earth Science

ORIGINAL RESEARCH
published: 12 July 2021
doi: 10.3389/feart.2021.667501

Recent Seismicity in the Area of the Major, 1908 Messina Straits Earthquake, South Italy

Giancarlo Neri, Barbara Orecchio, Debora Presti, Silvia Scolaro and Cristina Totaro*

Department of Mathematics, Computer Sciences, Physics, and Earth Sciences, University of Messina, Messina, Italy

High-quality non-linear hypocenter locations and waveform inversion focal mechanisms of recent, shallow earthquakes of the Messina Straits have allowed us to obtain the following main results: 1) seismicity has occurred below the east-dipping north-striking fault proposed by most investigators as the source of the 1908, magnitude 7.1 Messina earthquake, while it has been substantially absent in correspondence of the fault and above it; 2) earthquake locations and related strain space distributions do not exhibit well defined trends reflecting specific faults but they mark the existence of seismogenic rock volumes below the 1908 fault representing primary weakness zones of a quite fractured medium; 3) focal mechanisms reveal normal and right-lateral faulting in the Straits, reverse faulting at the southern border of it (Ionian sea south of the Ionian fault), and normal faulting at the northern border (southeastern Tyrrhenian sea offshore southern Calabria); 4) these faulting regimes are compatible with the transitional character of the Messina Straits between the zone of rollback of the in-depth continuous Ionian subducting slab (southern Calabria) and the collisional zone where the subduction slab did already undergo detachment (southwest of the Ionian fault); 5) the whole seismicity of the study area, including also the less recent earthquakes analyzed by previous workers, is compared to patterns of geodetic horizontal strain and uplift rates available from the literature. We believe that the joint action of Africa-Europe plate convergence and rollback of the Ionian subducting slab plays a primary role as regard to the local dynamics and seismicity of the Messina Straits area. At the same time, low horizontal strain rates and large spatial variations of uplift rate observed in this area of strong normal-faulting earthquakes lead us to include a new preliminary hypothesis of deep-seated sources concurring to local vertical dynamics into the current debate on the geodynamics of the study region.

Keywords: hypocenter locations, focal mechanisms, earthquake source, regional geodynamics, messina straits, Italy

OPEN ACCESS

Edited by:
Claudia Piromallo, Istituto Nazionale di Geofisica e Vulcanologia (INGV), Italy

Reviewed by:
Simone Cesca, Helmholtz Centre Potsdam, Germany
Gianfranco Vannucci, Istituto Nazionale di Geofisica e Vulcanologia (INGV), Italy

****Correspondence:***
Debora Presti
dpresti@unime.it

Specialty section:
This article was submitted to Solid Earth Geophysics, a section of the journal Frontiers in Earth Science

Received: *13 February 2021*
Accepted: *24 June 2021*
Published: *12 July 2021*

Citation:
Neri G, Orecchio B, Presti D, Scolaro S and Totaro C (2021) Recent Seismicity in the Area of the Major, 1908 Messina Straits Earthquake, South Italy. Front. Earth Sci. 9:667501. doi: 10.3389/feart.2021.667501

PREMISE

The Messina Straits area is well known to be one of the areas with the highest seismic risk in the Mediterranean region. The December 28, 1908 earthquake was one of the most devastating seisms of the past century with huge damage and 80,000 fatalities in Northeastern Sicily and Southern Calabria. Other major seisms which occurred in the previous centuries in Southern Calabria (February 1783) and Southeastern Sicily (January 1693) have also produced remarkable damage and victims on both sides of the Messina Straits.

Many geophysical and geological investigations have been performed on the 1908 earthquake with the purpose of identifying its source and relationship with the regional geodynamics. As discussed in a later Section, the intense efforts made by the scientific community to retrieve the source properties from the geodetic and seismic data available for the earthquake have allowed to obtain a family of solutions lying in an acceptably limited range concerning location, geometry and mechanism of the generating fault. The most convincing source appears to be a normal fault striking between N10W and NNE, east-dipping with a relatively low dip angle around 40°, and with the top located a few km beneath the Sicilian side of the Straits and the bottom beneath the Calabrian side (De Natale and Pingue, 1987; De Natale and Pingue, 1991; Capuano et al., 1988; Boschi et al., 1989; Bottari et al., 1989; Amoruso et al., 2002; Amoruso et al., 2006).

In the present study we analyze the local seismic activity recorded in the last twenty years in the Messina Straits area. We take benefit of the seismic network improvements occurred in this area during the 90's of the last century, making good databases available to researchers interested in high resolution analyses of local seismicity (Amato and Mele, 2008). We also take benefit of 1) recent improvements of algorithms for hypocenter location (Presti et al., 2004 and Presti et al., 2008) and focal mechanism computation (D'Amico et al., 2010 and D'Amico et al., 2011) and 2) increasing accuracy of the seismic velocity structure of this region (Neri et al., 2012; among others). On these grounds, we have started the present work confident to be able to furnish incremental knowledge on the seismicity of this area and relationships with the regional geodynamics.

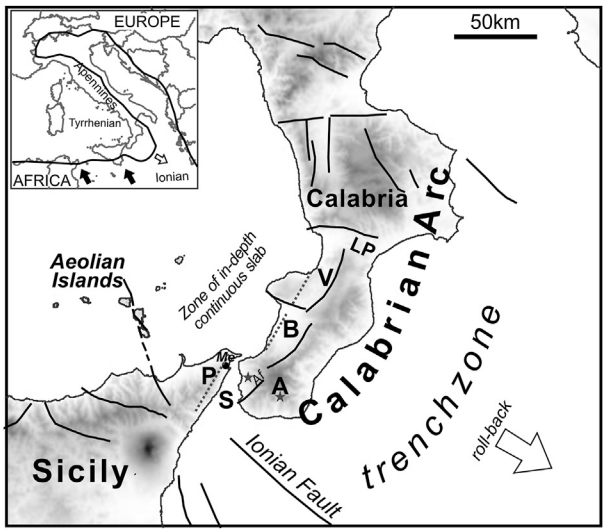

FIGURE 1 | Geodynamic sketch with main fault systems and topography of the Calabrian Arc region. In the upper-left inset, a simplified representation of the plate margin in the central Mediterranean region (black line) is shown. Full arrows indicate the present-day Africa motion with respect to Europe according to Nocquet (2012), and references therein. The white arrow in the main plate shows the sense of the gravity-induced subducting slab rollback. The dotted segments in the southern Calabria and Messina Straits area indicate the east-dipping blind faults proposed by several authors (see, e.g., DISS Working Group, 2018) as the seismogenic sources of the strong earthquakes of December 28, 1908 and February 5 and 7, 1783 discussed in the text. The stars indicate the epicenters of the 1908 Messina Straits and 1978 Aspromonte earthquakes according to Rovida et al. (2020) and Orecchio et al. (2019), respectively. A = Aspromonte, Af = Armo fault, B = Gioia Basin, Me = Messina,P=Peloritani, S = Messina Straits, V = Mesima Valley, LP = Lamezia Plain.

THE MESSINA STRAITS IN THE CALABRIAN ARC GEODYNAMIC FRAMEWORK

We have described the main geodynamic features of the Calabrian Arc region in previous studies, to which we address the reader interested in more details on the argument (see, e.g., Presti et al., 2013; Orecchio et al., 2015; Presti, 2020). Useful references may also be the basic continental-scale geodynamic reconstructions by Malinverno and Ryan (1986), Faccenna et al. (1996), and Rosenbaum et al. (2002). A widely shared geodynamic model of the Calabrian Arc region assumes the co-existence of 1) NNW–SSE convergence of Africa and Europe plates and 2) gravity-induced south-eastward rollback of a Ionian lithospheric slab subducting to northwest beneath the Tyrrhenian lithosphere (**Figure 1**). Plate convergence velocity is of the order of 3–5 mm/yr (see, e.g., D'Agostino and Selvaggi, 2004; Devoti et al., 2008), rollback of the subducting slab is also very slow (a couple of mm/yr; see, e.g., Hollestein et al., 2003; Devoti et al., 2008; Nocquet, 2012).

The Calabrian Arc presents strongly contrasting vertical movements, such as mountain chain uplifting of the order of 1–2 mm/yr since Middle Pleistocene and relative-to-chain subsidence in the major tectonic basins located on the western side of the chain (**Figure 1**; Monaco et al., 1996; Ferranti et al., 2007; Ferranti et al., 2010; Faccenna et al., 2011). Focusing on the Calabrian side of the Messina Straits area, Ferranti et al. (2007) estimated that the Late Holocene uplift is equally partitioned between steady and stick-slip coseismic contributions. On their hand, Ferranti et al. (2010) suggested a deep-seated contribution to remarkable uplift of Calabria, based on spatial correspondence between the uplifting area and the location of the Ionian subducting slab. It is worth mentioning that in the early phase of the debate on the Calabrian uplift, Negredo et al. (1999) proved by Finite Element Modeling that coexistence of plate convergence and roll-back of an in-depth continuous subducting slab beneath the Calabrian Arc is compatible with chain uplift observed in Calabria. More recently, strong spatial variation of vertical movements in the Arc area was detected by GPS data (Serpelloni et al., 2013) with maximum uplift rate into the chain and maximum subsidence into the basins.

Normal faults located around the basins west of the chain are considered to be major seismogenic faults, with particular reference to the NE-trending fault systems of the Messina Straits, Gioia Basin and Mesima Valley (S, B and V in **Figure 1**). It can be remarked that the strongest earthquakes of the S, B and V basins of **Figure 1** (magnitude 7.1 of Dec 28, 1908 in S; magnitude 7.1 of Feb 5, 1783 in B; and magnitude 6.7. of Feb 7, 1783 in V) have been imputed to west-dipping faults located on the eastern border of the basin by

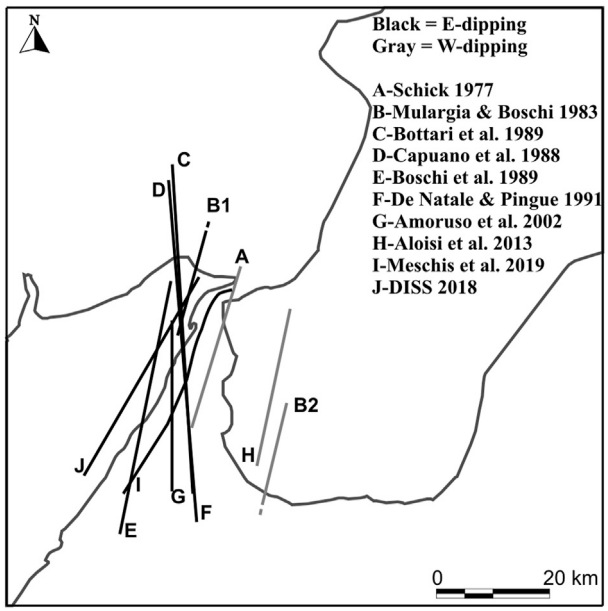

FIGURE 2 | Graphical summary of the sources proposed by different authors for the 1908 Messina Straits earthquake (legend). The traces A–J corresponding to the different sources indicate the intersection of the prolongation of the respective sources (fault planes) with the earth surface. Black and gray lines indicate E-dipping and W-dipping sources, respectively.

some authors (e.g. Monaco and Tortorici, 2000; Jacques et al., 2001) and to east-dipping faults on the western border of the basin by others (e.g. Valensise and D'Addezio, 1994; Pizzino et al., 2004; DISS Working Group, 2018).

Analyses of different geophysical data have led Neri et al. (2009) and Neri et al. (2012) to propose that the Ionian subducting slab is still continuous over depth beneath the central part of Calabrian Arc (southern Calabria, between Messina Straits and Lamezia Plain; **Figure 1**), while detachment of the deepest portion of subducting lithosphere has already occurred beneath the Arc edges, i.e. beneath Northern Calabria (north of Lamezia Plain) and Northeastern Sicily (southwest of Messina Straits), respectively. The Messina Straits area (**Figure 1**) is transitional between the zone of rollback of the in-depth continuous Ionian subducting slab (southern Calabria) and the collisional zone where the subduction slab did already undergo detachment, southwest of the Ionian fault zone (Neri et al., 2012; Totaro et al., 2016; among others). In contrast to the mentioned spatial variation of vertical movements, the Southern Calabria Messina Straits area is characterized by quite low values of horizontal strain rate, of the order of 0–15 nanostrain/yr (Palano, 2015).

THE SOURCE OF THE 1908 EARTHQUAKE

In the first paper of the most recent epoch of seismological research concerning the 1908 earthquake source, Schick (1977) proposed a fault located in the middle of the Messina Straits, with a strike approximately along a north-south direction and dipping to the west (**Figure 2**). This conclusion was partly based on an analysis only qualitative of the original geodetic data gathered by Loperfido (1909) who measured vertical displacements on both sides of the Straits between two campaigns performed before and soon after the December 28, 1908 earthquake, respectively.

Mulargia and Boschi (1983) presented a graben-shaped model assuming that the earthquake was generated by joint activation of two faults, a east-dipping one with top between the Sicilian side of the Straits and a west-dipping one with top beneath the Calabrian side (B1 and B2 in **Figure 2**).

The studies that followed demonstrated that a single east-dipping fault located in the middle of the Straits may explain the main features of the levelling data (De Natale and Pingue, 1987; De Natale and Pingue, 1991; Capuano et al., 1988; Boschi et al., 1989; Bottari et al., 1989; Amoruso et al., 2002; Amoruso et al., 2006). The source models proposed by these authors differed one from the other in terms of the fault length and small differences in strike orientation between N10°W and NNE. All analyses, whether seismological or geodetic or joint seismological/geodetic, indicated normal faulting.

Valensise and Pantosti (1992) and D'Addezio et al. (1993) analyzed recent geologic and geomorphic features on both sides of the Messina Straits and compared the distribution and deformation patterns with the displacement fields produced by different fault models that were proposed by several authors for the 1908 earthquake. They concluded that the long-term evolution of the Straits is strongly affected by the repetition of coseismic deformation episodes related to the occurrence of 1908 –type earthquakes represented by Boschi et al.'s (1989) NNE-trending east-dipping source. A main product of these investigations is the 1908 earthquake source reported in the Database of Individual Seismogenic Sources (DISS Working Group, 2018).

By analysis of the original seismograms, Pino et al. (2000) inferred that the 1908 earthquake was generated by unilateral rupture, with northwards directivity along a 43-km-long fault in the Straits. The extensional nature of the faulting, which involved rupturing of a roughly N-S striking plane, was confirmed.

A nonlinear joint inversion of P wave first-motion polarities and coseismic surface displacement data of the great earthquake allowed Amoruso et al. (2002) to propose a very stable solution according to which the earthquake was generated by a fault oriented ca. N-S located beneath the Straits, dipping to east at an angle of 40° and characterized by normal mechanism with a minor dextral lateral component.

In a more recent paper, Aloisi et al. (2013) proposed that the original levelling data do not allow reliable discrimination of the fault plane and claimed that an antithetic plane dipping westwards at a high angle provides an almost equivalent solution. Based on geological considerations, they suggested the Armo fault, located on-shore east of the Straits in Southern Calabria (**Figure 1**), as the source of the 1908 earthquake. They argued that southern Calabria represents the locus of major deformation in the region and reported on the

documented activity of the Armo fault during the late Holocene. Nevertheless, they did not provide any element that demonstrates that the only 18-km long Armo fault was activated during the 1908 earthquake. Some inconsistencies in this study were, however, contested by De Natale and Pino (2014) concerning, in particular, the use of the levelling data.

Convertito and Pino (2014) tested three typologies of sources among those proposed in the literature (Boschi et al., 1989; De Natale and Pingue, 1991; Aloisi et al., 2013) by computing synthetic seismograms from the respective sources and comparing the PGA and PGV values to the macroseismic intensity field available for the earthquake. They concluded that, among the tested models, the one characterized by an east-dipping fault, with strike oriented NS slightly rotated clockwise, better explains the observed macroseismic field of the 1908 Messina Straits earthquake. Then, they identified the fault proposed by Boschi et al. (1989) as the best fitting one.

In the last years several efforts have been made to find evidence of the 1908 earthquake source on the sea bottom of the Messina Straits. High-resolution swath bathymetry of the Messina Straits has led Ridente et al. (2014) to conclude that intense erosional and depositional processes superimposed on active tectonic deformation hinder the distinction between tectonic and sedimentary features, so that fault systems compatible with the source of the 1908 earthquake could not be identified. Based on multibeam sonar, chip profiler and seismic reflection data, Goswami et al. (2014) explored the seabed morphology of the Messina Straits and detected mass wasting processes around fault escarpments previously identified by Selli et al. (1978) on the Calabrian side of the Straits. No conclusion was, however, drawn in this connection concerning eventual seismic activity. More recently, Fu et al. (2017) discovered a major east-trending fault zone at the southern border of the Messina Straits, highlighted by a prominent 60 m high escarpment on the Ionian seafloor. Fu et al. (2017) proposed this fault zone as a potential source of seismic and tsunami hazard, but they excluded a role of it as source of the 1908 earthquake for incompatibility with the seismic data of this earthquake.

A couple of years ago, Meschis et al. (2019) tested the compatibility between the IGM levelling data of Loperfido (1909) with the NNE-SSW fault (I in **Figure 2**) reported by Doglioni et al. (2012) on the basis of geomorphic elements and acoustic data obtained by previous investigators in the Ionian offshore of Northeastern Sicily. Meschis et al. (2019) found the best fit of levelling data with this fault when assuming a east-ward dip of 70° and 5 m of maximum slip at depth. The authors have not, however, compared their source with the seismic data. Finally, during the phase of revision of the present article, a new paper appeared in the literature (Barreca et al., 2021) proposing a NNE-trending SE-dipping fault in the Messina Straits as the source of the 1908 earthquake, with the peculiar feature of a northeast-ward rotation of the northernmost part of the fault and possible continuation across southern Calabria mainland.

On the basis of the wide series of studies available in the literature, the largely most convincing source of the 1908 Messina Straits earthquake appears to be a low-angle east-dipping normal fault striking between N10W and NNE, with the top located a few km beneath the Sicilian side of the Straits. Analogue modeling allowed Bonini et al. (2011) to state that high-angle, very shallow normal faults detected over all the Messina Straits area can be interpreted as minor structures related to the activity of this low-angle east-dipping, deeper normal fault believed to have generated the 1908 earthquake.

METHODS OF ANALYSIS, DATA AND RESULTS

We perform estimates of hypocenter locations in the present study by the Bayloc Bayesian non-linear location algorithm (Presti et al., 2004 and Presti et al., 2008). Starting from seismic phase arrival times at the recording stations, Bayloc computes for an individual earthquake a probability cloud marking the hypocenter location uncertainty and defines the point-location of the earthquake as the point of maximum probability in the cloud. Then, Bayloc estimates the spatial distribution of probability relative to a set of earthquakes by summing the probability densities of the individual events. This procedure has been shown to help detection of seismogenic structures through better hypocenter location and more accurate estimation of location errors compared to linearized methods (Presti et al., 2008). More details on methodological aspects of Bayloc can be found in Presti et al. (2004) and Presti et al. (2008).

We have applied Bayloc to the earthquakes of magnitude greater than two occurred at depth less than 30 km in the area of **Figures 3A–C** during the period 2000–2020. We have taken the P- and S-wave arrival times of these earthquakes from the Italian national seismic database (http://terremoti.ingv.it/) and selected the subset of earthquakes for which a minimum of six P-wave arrival times at stations with epicentral distance <150 km were available. A map of the stations used for these hypocenter locations is shown in **Figure 3D**. The 3D velocity model estimated for the study area and surroundings by Neri et al. (2012) has been used for locations. Based on completeness analyses of the seismic database performed by previous authors (Schorlemmer et al., 2010), we are confident that our sample of shallow earthquakes of magnitude over 2.0 in the Messina Straits area is substantially complete. The results of our hypocenter locations are shown in the maps of **Figures 3A–C**, reporting the cumulative probability density of the earthquakes (A), the corresponding point-locations (B) and the seismic energy density relative to plot A (C). With the same types of representation, the **Figure 4** reports the maps (A, C and E) and the W-E vertical sections (B, D and F) of the seismicity located in the sector of the 1908 earthquake source. All plots A-to-F show the trace of the 1908 earthquake fault of Amoruso et al. (2002), more precisely the intersection of the prolongation of the fault with the earth surface is reported in the map views. In addition, the low-right insets in the plots C and D of **Figure 4** show the Bayloc's barycentric distributions representing the average uncertainty volume of the located earthquakes in the map and section views (Presti et al., 2008). The relatively small

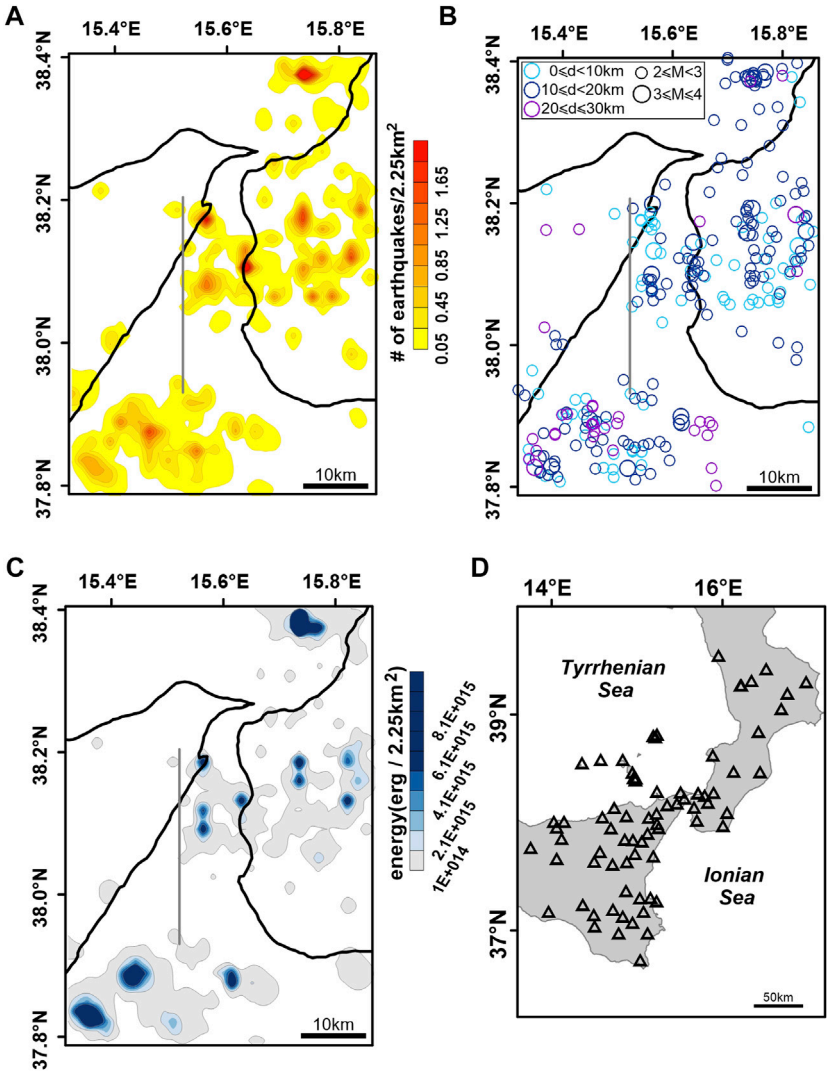

FIGURE 3 | Epicentral maps obtained by the Bayloc probabilistic location method for M ≥ 2 earthquakes occurred at depth less than 30 km in the period 2000–2020. For comparison, the 1908 earthquake source of Amoruso et al. (2002) is reported in plots A-to-C (gray line): the trace corresponds to the intersection between the fault plane prolongation and the earth surface. Bayloc locations are reported both in terms of cumulative probability density **(A)** and point-locations, i.e. points of maximum probability **(B)**. The graphical representation in plot **(B)** allows for differentiation of earthquakes according to depth d and magnitude M (legend). Plots **(C)** and **(D)** show the seismic energy density relative to plot A and a map of the stations used for hypocenter locations, respectively.

extent of the average uncertainty volume of hypocenters, corresponding to ERH and ERZ values of the order of 0.7 and 1 km, respectively, represent a basic pre-condition for the forthcoming analysis and discussion of the earthquake space distributions. Finally, **Figure 5** displays the cross-section views of the hypocenters of earthquakes of **Figure 4** along profiles perpendicular to the orientations of the east-dipping sources of the 1908 earthquake proposed by different authors (Boschi et al., 1989; De Natale and Pingue, 1991; Amoruso et al., 2002; DISS Working Group, 2018). This family of east-dipping sources is here intended as a sort of range of uncertainty of the 1908 source.

Hypocenter locations obtained by Bayloc have been used as starting data for computation of focal mechanisms. For this, we have used the Cut and Paste (CAP) waveform inversion method by Zhao and Helmberger (1994), and Zhu and Helmberger (1996). Each waveform is broken up into Pnl and surface wave segments, which are given different weights during inversion. The same frequency bands have been used to filter synthetic and observed ground velocities, in detail 0.02–0.1 Hz for surface waves and 0.05–0.3 Hz for Pnl waves. Diversely from other waveform inversion methods of current use in the literature which are known to be effective when the earthquake magnitude exceeds a threshold of 3.5–4 (Pondrelli et al., 2006; Ekstrom et al., 2012), CAP has shown to be very effective also for earthquakes of magnitude in the range 2.5–3.5 (more details on CAP and its applications can be found in Zhao and Helmberger, 1994; Zhu and Helmberger, 1996; D'Amico et al., 2010; D'Amico et al., 2011; Scolaro et al., 2018).

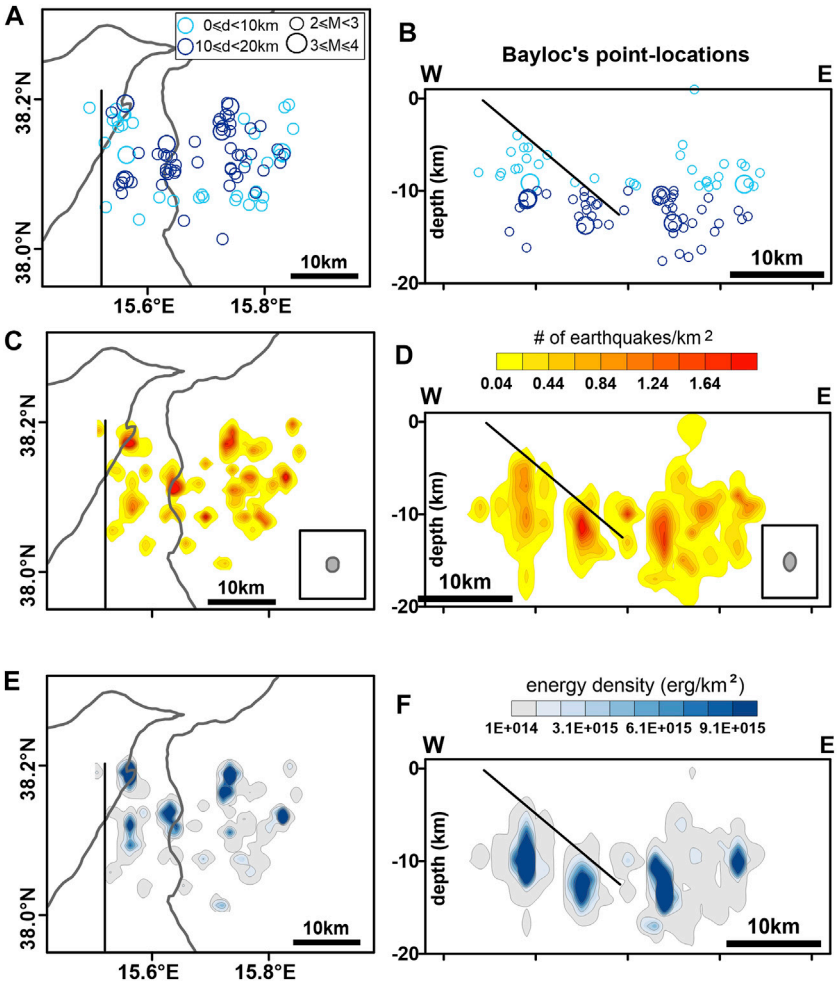

FIGURE 4 | Epicentral maps (left) and E-W oriented vertical sections (right) of recent earthquakes located in the sector of the 1908 earthquake source. For comparison, the 1908 earthquake source of Amoruso et al. (2002) is reported in all plots (black line): in the maps the trace corresponds to the intersection between the fault plane prolongation and the earth surface, in the vertical sections the trace shows the location of the circa north-striking east-dipping source. Top **(A–B)**: earthquake point-locations with differentiation of earthquakes according to depth d and magnitude M (legend). Middle **(C–D)**: distribution of the cumulative probability density. The average epicentre and hypocentre uncertainties expressed in terms of "barycentric map" and "barycentric vertical section" (see text, and Presti et al., 2008) are also reported in the low-right insets of C and D plots. Bottom **(E–F)**: seismic energy density distribution. All the earthquakes reported in the maps **(A,C,E)** are projected onto the cross-sections **(B,D,F)**.

We have applied the CAP method to seismic waveforms available in the database EIDA, http://orfeus-eu.org/webdc3/, for the shallow earthquakes that occurred in the study area since 2005. A greater number of waveforms is generally available in the database for the most recent earthquakes, and this has led us to obtain well constrained solutions in large majority for earthquakes occurred in the last few years. The earth structure used for the Green's Functions computation was properly calibrated for the study area by D'Amico et al. (2011). The most stable focal mechanisms obtained by CAP in the present study are reported in **Figure 6** and **Table 1**. The stability of the solutions has been carefully checked by means of tests and procedures widely described in D'Amico et al. (2011) and Scolaro et al. (2018). For conciseness, we report in **Figures 7A–D** the comparison between synthetic and observed waveforms relative to the earthquakes n. 1, 5, 10 and 14 of **Figure 6** sampling the different sectors of the study area. An overally good fit of waveforms can be observed at almost all the recording stations, the map of which is given in **Figure 6**. In addition to the best solution obtained for the individual earthquake, each of the four sections of **Figures 7A–D** reports in the top the solutions obtained by moving the hypocenter of the event in all directions within the Bayloc's uncertainty volume of the event itself. The focal mechanisms of the events 1, 5, 10 and 14 appear very stable. Similar levels of stability have been obtained for the other events of **Figure 6**. Finally, we note that the earthquake of October 6, 2006 in **Table 1** (n. 13) was also present in the list of earthquakes analysed in the previous paper by Presti et al. (2013), indicated as n. 97 in their **Table 1** and **Figure 4**. Slight differences of fault parameters between the respective solutions, resulting from difference between

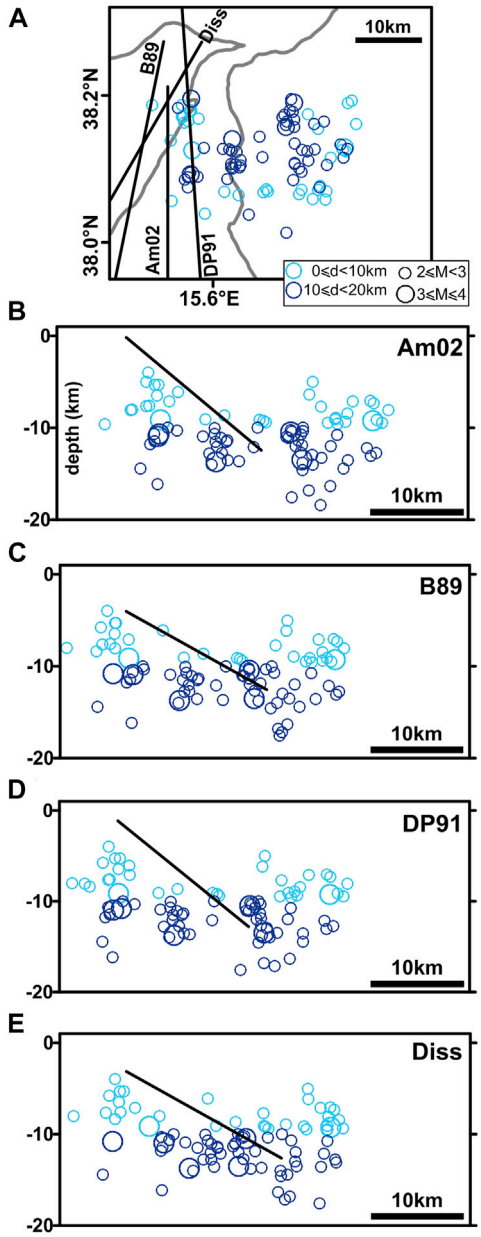

FIGURE 5 | Plot **(A)** reproduces the epicentral map of **Figure 4A** reporting also the traces of the east-dipping sources of the 1908 earthquake proposed by different authors: Am02, B89, DP91 and Diss stand for Amoruso et al. (2002), Boschi et al. (1989), De Natale and Pingue (1991) and DISS Working Group (2018), respectively. Plots B-to-E display the cross-section views of the earthquakes of plot **(A)** along profiles perpendicular to the orientations of the different sources. All the earthquakes reported in the map **(A)** are projected onto the cross-sections **(B–E)**. This family of east-dipping sources is here intended as a sort of range of uncertainty of the 1908 source.

1) Bayloc's earthquake location used for CAP inversion in the present study and 2) Italian bulletin's earthquake location used for CAP estimates reported in Presti et al. (2013), highlight substantial stability of this mechanism also varying the location of the event according to different procedures.

DISCUSSION

Figure 3 shows the epicenter map of the earthquakes shallower than 30 km which occurred in the Messina Straits area during the last 20 years. Seismicity has been mainly located in the Straits, in the Calabrian on-shore east of it, and in two offshore sectors located NE and SW of it, respectively. A maximum magnitude of 4.0 has been recorded in the whole area during the study period. A quite low seismicity level (both as number and energy of earthquakes) was recorded on the Sicilian on-shore of the Straits. Higher and lower activity recorded on the Calabrian

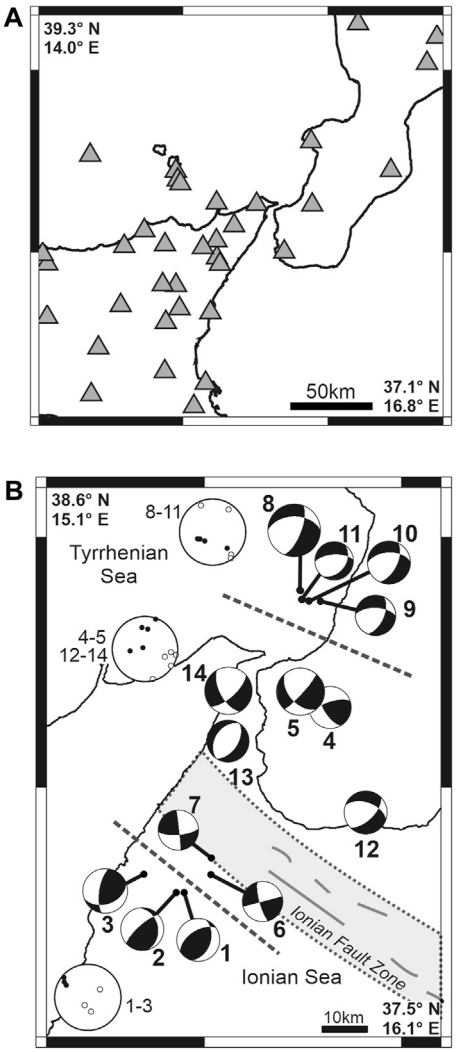

FIGURE 6 | (A) Seismic stations used for focal mechanism computations. **(B)** Waveform inversion focal mechanisms computed by the CAP method for earthquakes occurred at depths less than 30 km in the Messina Straits area between 2005 and 2020. Numerical values of earthquake parameters are reported in **Table 1**. Polar plots of P- and T-axes for three different subsets of our FMs (1–3; 4–5 and 12–14; 8–11) are also reported, with the standard representation black = P and white = T. Dashed lines help recognizing the different compartments discussed in the text. The NW-SE striking gray belt in the Ionian Sea shows the location of the Ionian Fault Zone (see Polonia et al., 2016, among others).

TABLE 1 | Identity number, date and origin time, hypocenter coordinates, fault parameters and moment magnitude of the earthquakes reported in **Figure 6**. The number of traces used for each focal mechanism computation is also reported in the last column.

ID	YYYY-MM-DD	hh:mm	sec	Lat (°N)	Lon (°E)	Depth (km)	Strike (°)	Dip (°)	Rake (°)	Mw	no. of traces
1	2015-12-22	02:13	39	37.79	15.45	18.11	19	42	60	3.3	12
2	2015-12-22	05:35	9	37.79	15.43	22.38	348	28	33	3.3	9
3	2016-02-11	01:38	50	37.83	15.35	26.87	189	68	56	3.4	4
4	2016-11-18	17:14	1	38.16	15.82	20.10	251	68	28	3.2	6
5	2018-02-10	02:16	17	38.19	15.75	12.64	42	82	−41	3.6	13
6	2018-02-27	12:35	13	37.83	15.52	14.74	255	90	13	3.1	6
7	2018-02-27	12:44	18	37.86	15.52	15.00	85	71	3	3.1	6
8	2018-09-28	05:24	31	38.40	15.74	17.00	269	46	−31	4.0	23
9	2018-10-03	01:23	1	38.37	15.79	20.72	272	59	−39	3.1	7
10	2018-11-14	15:01	2	38.37	15.76	18.00	267	51	−42	3.3	12
11	2018-11-14	15:15	3	38.38	15.75	18.00	267	63	−61	2.9	7
12	2019-08-14	23:26	22	37.95	15.91	16.00	289	51	−39	3.3	13
13	2006-10-06	21:16	23	38.09	15.56	11.00	33	51	−90	3.2	6
14	2013-12-23	04:20	38	38.19	15.56	11.00	48	67	−32	3.6	11

and Sicilian sides of the Straits, respectively, correspond to higher and lower degree of surface faulting and associated deformation (rate of geological moment release) estimated in the respective sectors by Ghisetti (1992). The **Figure 4** allows us to better focus on the seismicity located in the upper 20 km in the Straits and the Calabrian on-shore east of it, in particular we may look at the events occurring in the sector of the 1908 earthquake fault as reconstructed by Amoruso et al. (2002). All plots A-to-F in **Figure 4** show, in fact, the trace of Amoruso et al.'s 1908 earthquake fault, more precisely the trace in the map representations corresponds to the intersection between the fault plane prolongation and the earth surface. In the cross-section views, the trace shows the location of the circa north-striking east-dipping Amoruso et al.'s source. A striking feature appearing from **Figure 4** is that the recent seismicity occurred in the Straits is nearly all located below and east of the Amoruso et al.'s 1908 fault plane, with some events only located close above the bottom edge of the fault. This feature is highlighted by the great accuracy of hypocenter locations already discussed in the previous Section. Non-linear locations performed by the Bayloc algorithm, and the use of the robust dataset of the last 2 decades, have allowed us to obtain hypocenter distributions accurate enough for comparison between recent earthquake activity and the 1908 source. Less accurate locations performed with linearized methods applied to databases as long as 4 decades (including poorer network geometries) result in very noisy distributions of hypocenters (see, e.g., Barreca et al., 2021). The plots of **Figure 4** show also several clusters of earthquakes below the 1908 fault, more or less concentrated, but they do not display any clear evidence of trends indicating seismogenic faults. The findings of **Figure 4** suggest that a huge portion of the rock volume located above the 1908 fault is quite inactive from the seismic point of view. This could mean that the rock fracturing level is relatively low in it. The events located close above the bottom edge of the 1908 fault and east of it mark the (Calabrian) eastern boundary of the low-fractured block standing over the fault. **Figure 5** displays the hypocenter vertical sections of the recent seismicity occurred in the 1908 earthquake fault area, taken perpendicular to the orientations of the east-dipping sources proposed by different authors in the literature. The Figure shows that the conclusions drawn by comparing the recent earthquake locations to the location of the Amoruso et al. (2002) source of the 1908 earthquake are confirmed when considering the other sources, in particular most of the hanging wall of the 1908 fault is a low-fractured block.

The **Figure 6** displays the waveform inversion focal mechanisms estimated in the present study for the recent shallow earthquakes occurred in the study area of **Figure 3**. The figure shows reverse mechanisms at the southern border of the area (earthquakes n. 1–3), extensional ones at the northern border (8–11), and a mixture of extensional and right-lateral mechanisms in the Straits and the Calabrian on-shore of it (4–5 and 12–14). The earthquakes n. 6 and 7, located near the right-lateral Ionian fault zone corresponding to the southwestern edge of the Ionian subducting slab (shadowed belt in **Figure 6**; see also Polonia et al., 2016), show dextral strike-slip mechanisms compatible with the kinematics of same fault zone. The distribution of mechanisms of **Figure 6** (see also the polar plots of P and T axes relative to the different compartments) matches well with the geodynamic model of the study area assuming that the Messina Straits area is transitional between the zone of rollback of the in-depth continuous Ionian subducting slab (southern Calabria) and the collisional zone where the subduction slab did already undergo detachment (southwest of the Ionian fault zone) (Neri et al., 2012; Orecchio et al., 2014; among others). Normal faulting earthquakes in the Tyrrhenian sea offshore southern Calabria (FMs n. 8–11) are compatible with southeast-ward rollback and trench retreat of the subducting Ionian slab. Reverse mechanisms in the Ionian sea southwest of the Ionian fault zone (FMs n. 1–3) are compatible with the collisional domain existing southwest of the subducting slab edge. The transitional character of the Messina Straits implies reasonably the coexistence of normal faulting and right-lateral mechanisms, the latter accommodating the internal deformation of the overriding unit subjected to differential southeast-ward advance onto the subducting one (this mechanism is schematized

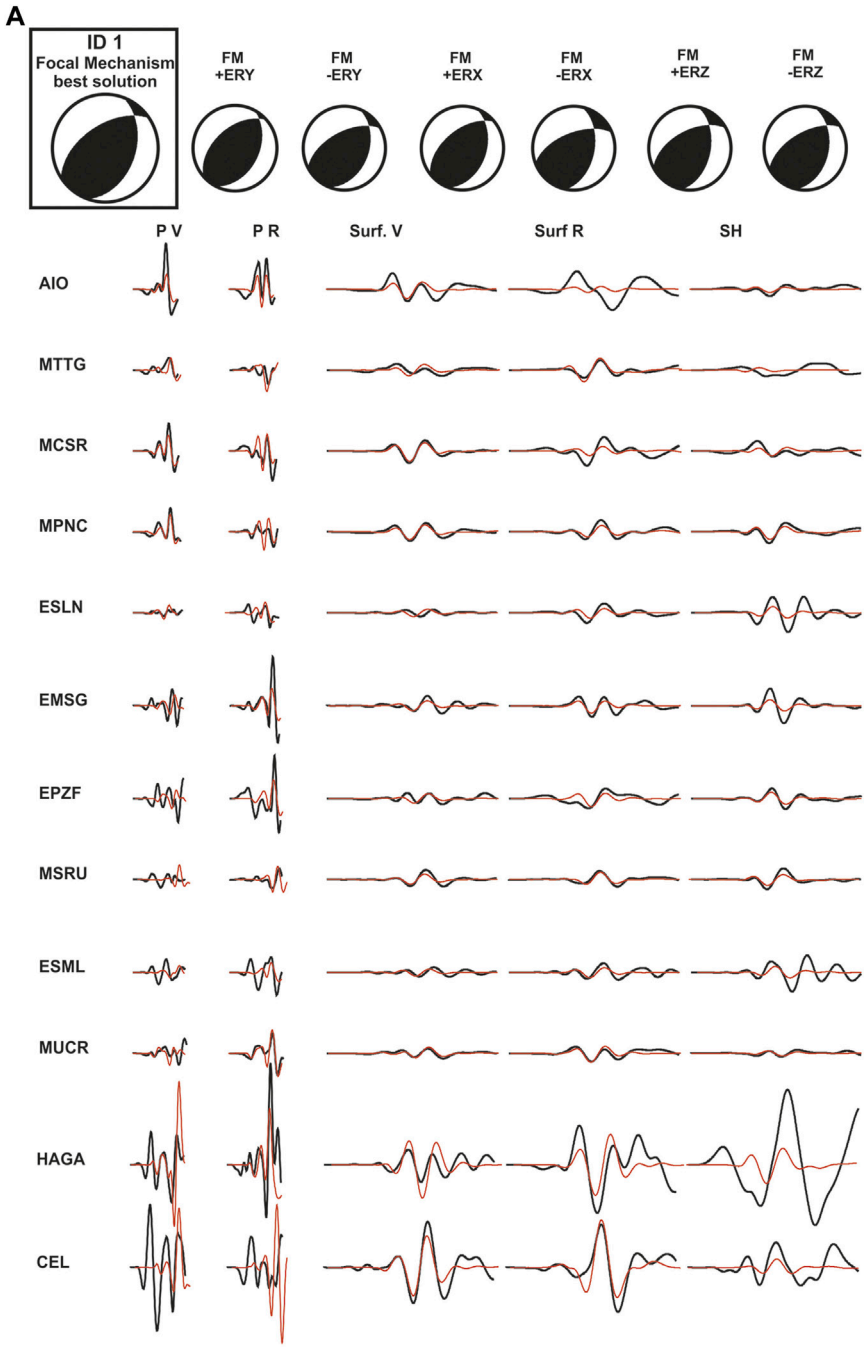

FIGURE 7 | Plots **(A–D)** show waveform inversion results obtained in the present study for the earthquakes n. 1, 5, 10 and 14 of **Figure 6** and **Table 1**. For each event we report the best focal mechanism solution (top-left, in the box), the relative waveform fits (observed-black vs predicted-red; main part of the figure), and some stability tests of the solution performed by moving the hypocenter in all directions within the Bayloc's uncertainty volume of the event itself (top of the plot, to the right of the best solution).

in the forthcoming **Figure 9A**). Coexistence of normal faulting and right-lateral mechanisms is just what we obtain in the present study by analysis of focal mechanisms in the Messina Straits and the Calabrian onshore east of it (FMs n. 4–5 and 12–14 in **Figure 6**). The quality of the focal mechanisms (some examples of stability tests are given in **Figure 7**) supports our interpretation of themselves in the frame of the above mentioned geodynamic model.

We show in **Figure 8A** the map of present-day uplift rate values reported by Serpelloni et al. (2013) for a ca. NW-trending rectangular sector including southern Calabria (south of Lamezia Plain) and the Messina Straits. The GPS stations used by

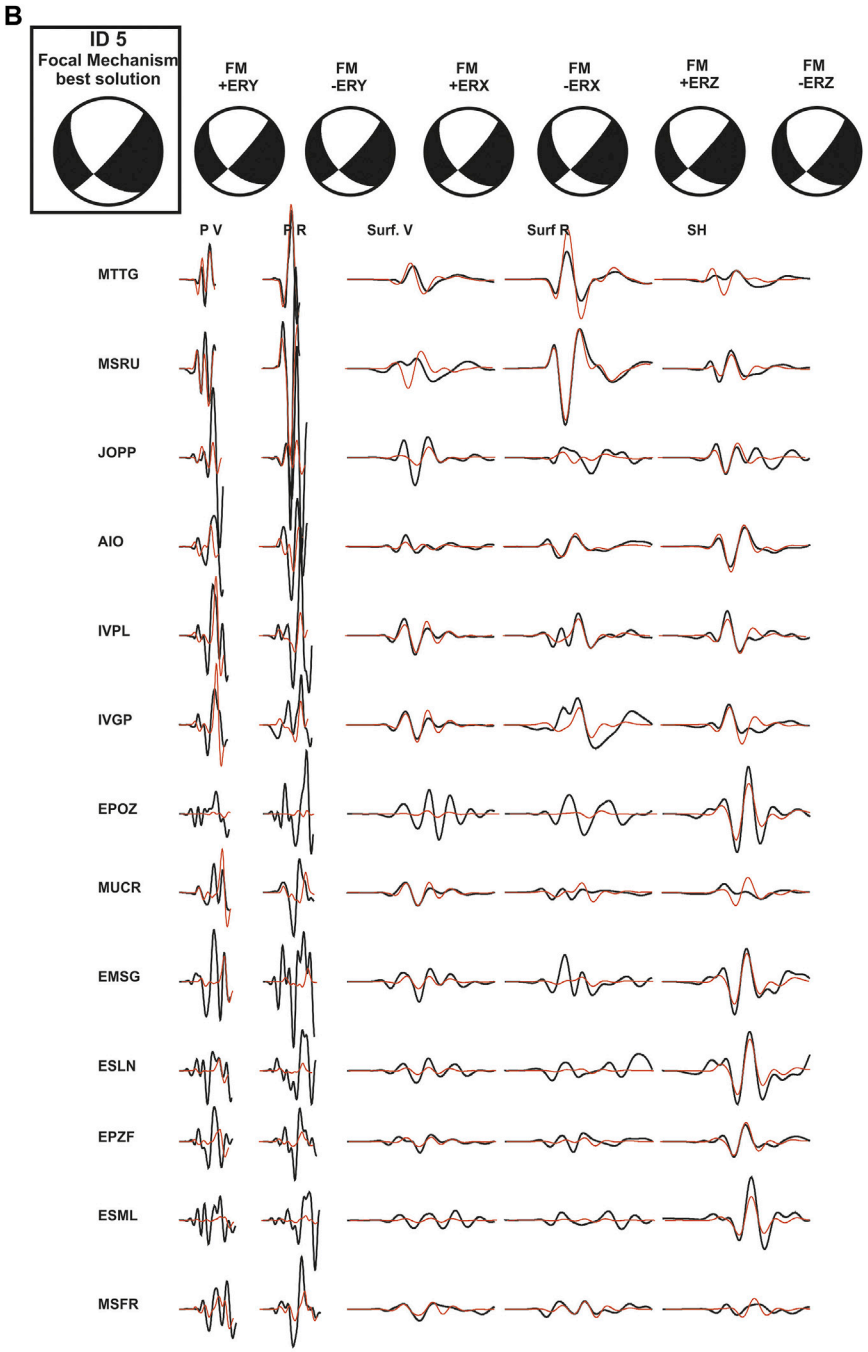

Figure 7. | (Continued).

Serpelloni et al. (2013) for their study are almost all concentrated in the southwestern half of the rectangle, more precisely in the sector of the Arc comprising the basins of Gioia Tauro and Messina Straits. We may consider the cross-section view of the same data (**Figure 8B**, taken from Serpelloni et al.'s Figure 13) as representative of the uplift rate pattern along profile crossing (from SE to NW) the Aspromonte chain, the basins (Gioia Tauro and Messina Straits), and the eastern Aeolian Islands in the southeastern Tyrrhenian sea. The profile of our **Figure 8B** (taken from Figure 13 of Serpelloni et al., 2013) shows the maximum value of uplift rate in southeastern Calabria (0.8 mm/yr; southeast of the top of the chain indicated by T) and a rapid drop to a minimum of—0.8 mm/yr moving to NW in the basins' area (Ba). Northwest of the minimum, the profile shows a NW-ward increasing uplift rate from—0.8 mm/yr to circa 0 mm/yr. This pattern indicates a SE-ward progressive subsidence in the

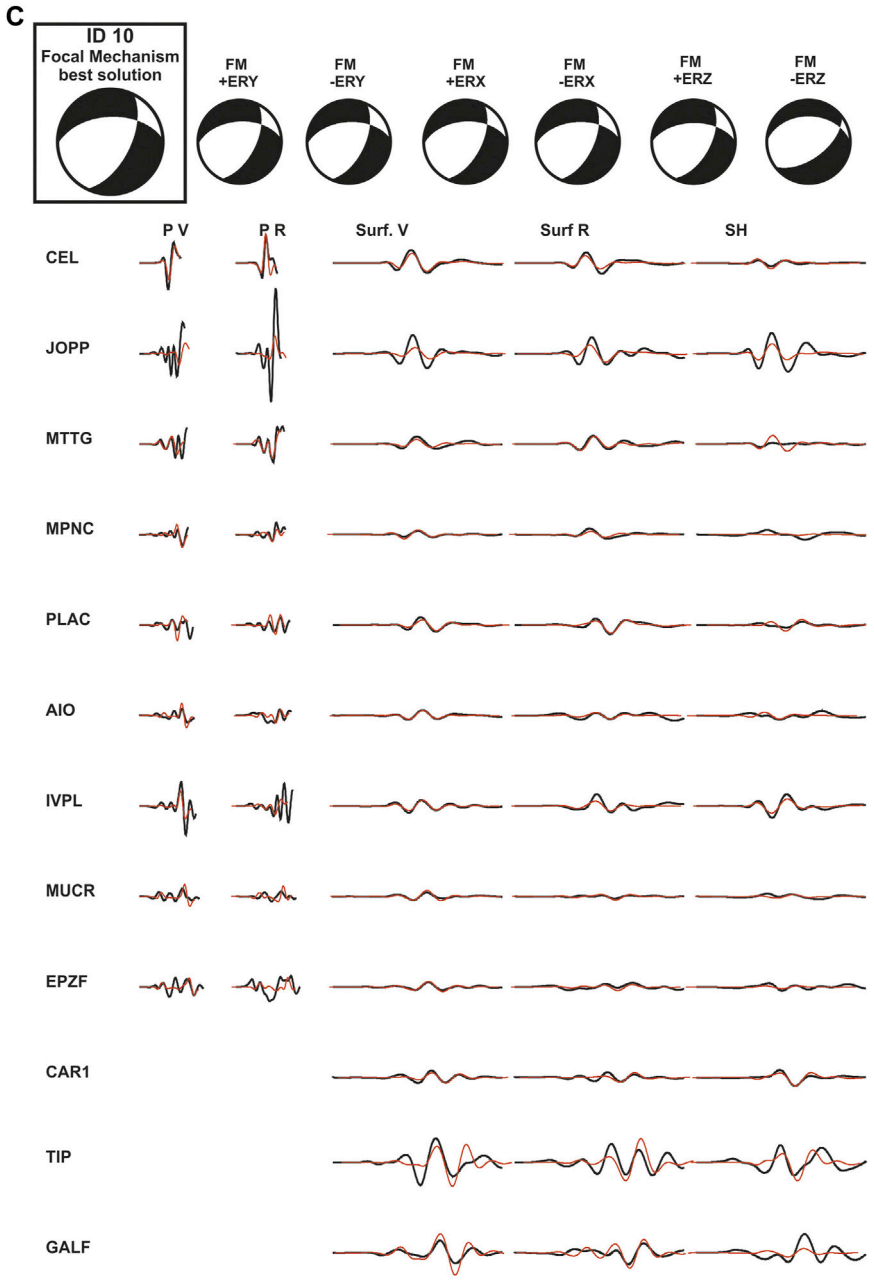

Figure 7. | (Continued).

area of the basins (Gioia Tauro and Messina Straits). Even if future data acquisition is needed for a more robust analysis of the uplift rate pattern in this area, in particular in the Messina Straits area, we take from Serpelloni et al.'s data a preliminary indication of a possible phenomenon of east-ward progressive subsidence in the Messina Straits. We may also note from **Figure 8** that 1) the maximum uplift rate of 0.8 mm/yr corresponds to the eastern boundary of the Aspromonte chain and 2) the rapid drop of uplift rate observed moving to NW contains the location (E) of the March 11, 1978, magnitude 4.7 earthquake investigated by Orecchio et al. (2019). For this earthquake, Orecchio et al. (2019) estimated a depth of 8 km and a normal-faulting mechanism on a high-dip NNE-trending fault plane dipping to WNW (**Figure 8C**). On the basis of these data, we tend to believe that the March 1978 Aspromonte earthquake may have derived from differential uplift into the chain area.

We suggest the following geodynamic processes to explain the findings of the present study concerning recent seismicity of the Messina Straits and the information available from literature concerning 1) the 1908 earthquake and 2) other geophysical features of the southern Calabrian Arc. A primary process is the

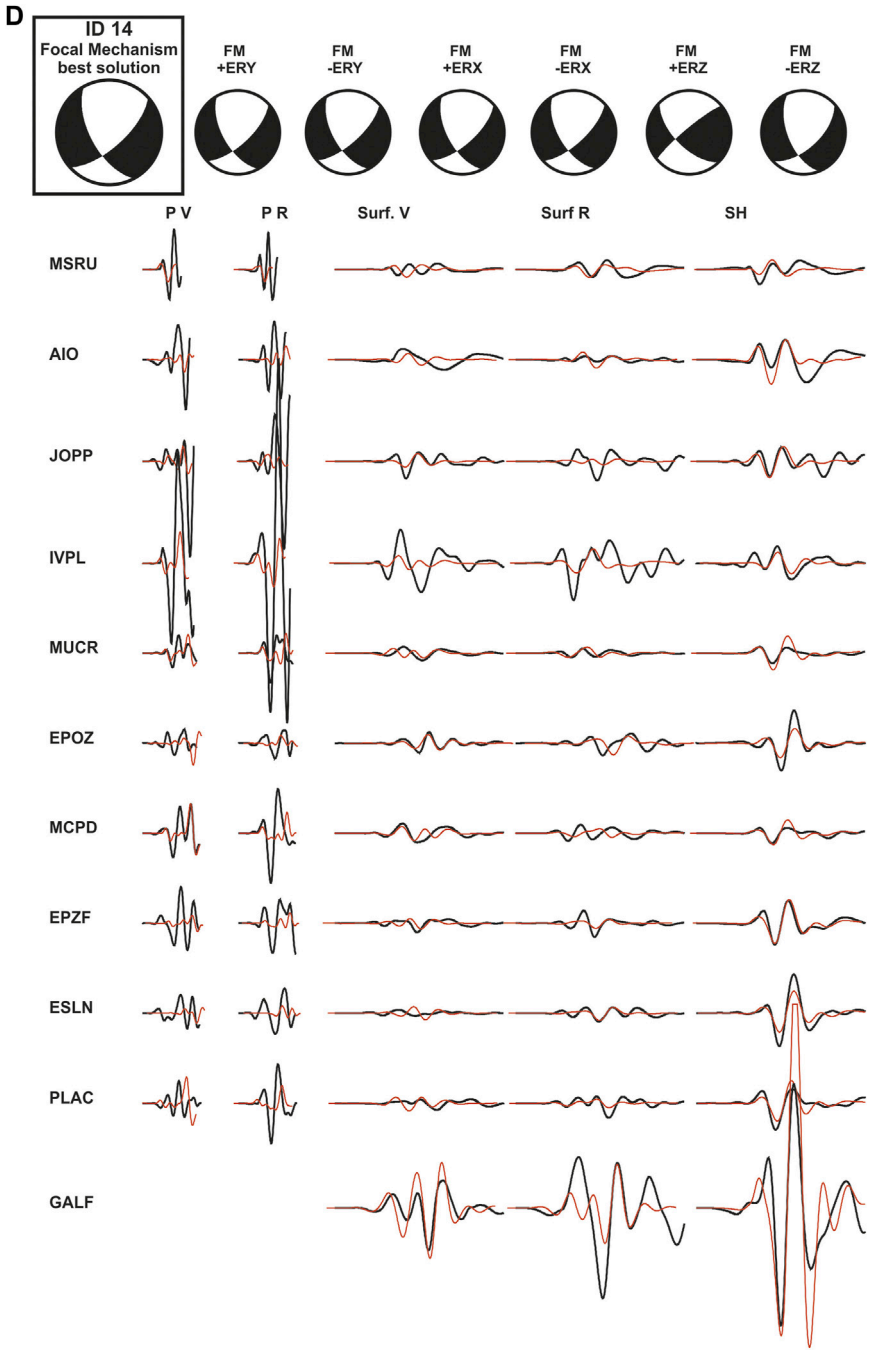

Figure 7. | (Continued).

widely shared coexistence in the study region of 1) Africa-Europe NNW-trending plate convergence and 2) SE-ward residual rollback of the Ionian lithospheric slab subducting underneath the Tyrrhenian-Calabria unit. As said above, the Messina Straits area can be considered as transitional between the zone of rollback of the in-depth continuous subducting slab (southern Calabria) and the collisional zone where the subduction slab did already undergo detachment (southwest of the Ionian fault zone) (Neri et al., 2012; Orecchio et al., 2014). This transitional character of Messina Straits would produce the observed coexistence of normal faulting and right-lateral mechanisms (**Figure 6**), the latter accommodating the internal deformation of the overriding unit due to the decreasing trench retreat when approaching the slab edge. As said in a previous Section, the coexistence of Africa-Europe convergence and rollback of the Ionian subducting lithosphere was shown to be able to produce

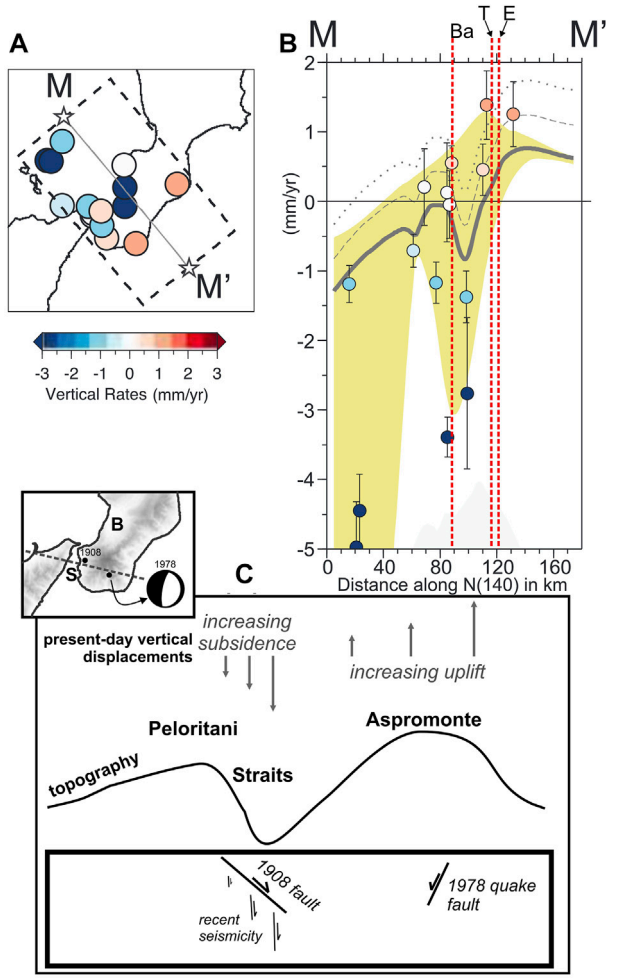

FIGURE 8 | Map plot **(A)** and related cross-section view plot **(B)** of the present-day uplift rate values estimated by Serpelloni et al. (2013) in a ca. NW-trending rectangular sector including southern Calabria and the Messina Straits (redrawn from Serpelloni et al., 2013). "Ba", "T" and "E" in the plot **(B)** indicate, respectively, the basins' area (Gioia Tauro basin and Messina Straits), the top of the mountain chain and the location of the 1978 Aspromonte earthquake. Serpelloni et al.' s (2013) gray curve indicating the uplift rate pattern along the MM' profile in plot **(B)** evidences that the maximum of the present-day uplift rate is located southeast of the top of the chain and of the 1978 Aspromonte earthquake. The plot **(C)** (with the inset showing the Aspromonte-Peloritani profile and the focal mechanism of the 1978 Aspromonte earthquake) furnishes sketch representations of 1) present-day vertical displacements across the Messina Straits area desumed from the patterns of plots **(A)** and **(B)**, 2) topography, and 3) the locations and kinematics of the faults which generated the earthquakes of 1908 (magnitude 7.1) and 1978 (magnitude 4.7). In the same plot **(C)**, "increasing subsidence" indicates the approximate location of the descending pattern of the gray curve that can be noted in the basin's area (Ba) in plot **(B)**, while "increasing uplift" marks the location of the gray curve growing pattern between the basin and the zone of maximum uplift rate. As explained in the text, future checks of these uplift/subsidence patterns should be performed by acquisition of new data especially in the offshore sectors.

uplift of southeastern Calabria (Negredo et al., 1999), and this is in agreement with Serpelloni et al.'s (2013) uplift rate pattern that we have reported in **Figure 8**. The above discussed phenomenon of east-ward progressive subsidence in the Messina Straits inferred from Serpelloni et al.'s uplift pattern reproduced in **Figure 8**, if it will confirmed in the future by a more robust

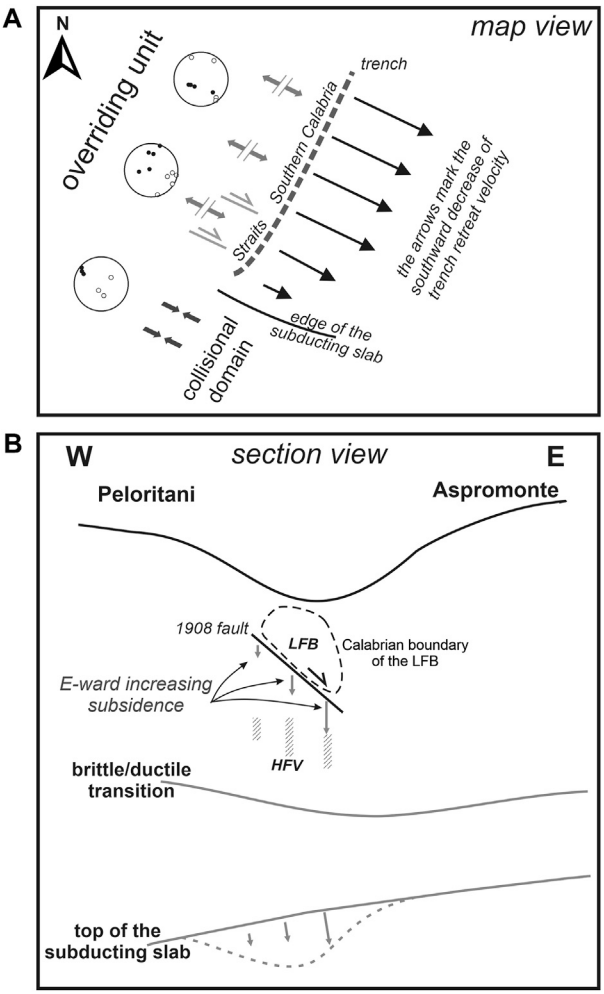

FIGURE 9 | Sketch representation of geodynamic engines producing seismicity in the Messina Straits area. The map view of plot **(A)** shows the progressive reduction of trench retreat velocity from northeast to southwest along the southern Calabrian Arc (southern Calabria–Straits) when approaching the southern edge of the Ionian subducting slab. This process produces internal deformation of the Messina Straits transitional zone between the extensional domain of southern Calabria and the collisional one of Sicily, southwest of the slab edge. Internal deformation of the Messina Straits is accommodated by dextral strike-slip mixed to normal faulting mechanisms (**Figure 6B**). The same polar plots of P- and T-axes reported in **Figure 6B** are also shown in this Figure for easier comparison. The representation of processes given in the section view of plot **(B)** is based on the preliminary evidence of east-ward progressive subsidence in the Messina Straits inferred from Serpelloni et al.'s (2013) uplift pattern reproduced in **Figure 8**. If this east-ward progressive subsidence will be confirmed in the future by new data including sea bottom measurements, this scheme will offer a new possible explanation of the loading mechanism of the 1908 fault. The east-ward increasing subsidence, eventually imputable to instabilities in the top of the subducting slab of the type suggested for the study region in previous papers (Orecchio et al., 2014; Presti et al., 2019), could drive the huge low-fractured block LFB resting on the fault to slide episodically onto the high-fractured volume HFV representing the footwall of the fault.

set of data including sea bottom measurements, could offer a new explanation of the loading mechanism of the 1908 fault. The east-ward increasing subsidence, eventually imputable to instabilities in the top of the subducting slab of the type suggested for the study region in previous papers (Orecchio et al., 2014; Presti et al., 2019), could drive the huge low-fractured block resting on the fault to slide episodically onto the more fractured basement representing the footwall of the fault (**Figure 9**). We offer this purely speculative hypothesis to the currently intense debate on local seismicity (Tiberti et al., 2017; Carafa et al., 2017; Presti et al., 2017; Neri et al., 2020; among others) and to future plans of data acquisition in the study region, also considering that vertical dynamics of the type suggested here would represent a simple and rather appropriate model for an area of strong normal-faulting earthquakes and relatively low horizontal strain rates like the Messina Straits.

CONCLUSION

The recent crustal seismicity in the area of the major, 1908 Messina Straits earthquake has mainly occurred below the east-dipping north-striking fault proposed by most investigators as the source of the 1908 earthquake, while it has been substantially absent in correspondence of the fault and above it (**Figures 4**, **5**). This distribution of seismicity suggests the existence of a huge, low-fractured shallow block resting on a somewhat fractured medium, with the separation surface between them roughly corresponding to the fault which generated the 1908 earthquake (**Figure 9B**).

The focal mechanisms of recent earthquakes (**Figure 6**) furnish a convincing picture of the transition from the extensional domain of southern Calabria (where southeast-ward trench retreat is still active, although slow) to the compressional domain of Sicily (where detachment of the subducting slab has already occurred), see **Figure 9A**. The progressive reduction of trench retreat from northeast to southwest produces internal deformation of the Messina Straits transitional zone and this deformation is accommodated by dextral strike-slip faulting mixed to normal faulting.

Starting from the above findings, we state that the joint action of Africa-Europe plate convergence and rollback of the Ionian subducting slab can be considered a major engine of seismicity in the Messina Straits area. A remarkable feature of the Messina Straits and the nearby southernmost Calabria is the occurrence of strong normal-faulting earthquakes (like 1908 and 1783) associated to evidence of relatively low horizontal strain rate furnished by GPS data of the last few decades (Palano, 2015). Different hypotheses have been proposed to explain this feature (Carafa et al., 2017; Presti et al., 2017; Tiberti et al., 2017; Neri et al., 2020). Starting also from strong spatial variations of geodetic uplift rate estimated by Serpelloni et al. (2013), we believe that hypotheses of deep-seated sources of stress concurring to local vertical dynamics (see, e.g., Orecchio et al., 2014) may reasonably be part of the ongoing debate on the study area. The apparent east-ward progressive subsidence in correspondence with the basin area (Serpelloni et al.'s Figures 10, 13 and our **Figure 8**), if confirmed in the future by acquisition of new data with particular reference to offshore areas, will furnish a new possible interpretation of the loading mechanism of the 1908 fault: the east-ward increasing subsidence would drive the huge low-fractured shallow block to slide episodically onto the more fractured basement in the Straits area (**Figure 9B**).

DATA AVAILABILITY STATEMENT

Publicly available datasets were analyzed in this study. These data can be found here: www.ingv.it; http://orfeus-eu.org/webdc3/.

AUTHOR CONTRIBUTIONS

GN and DP: coordination of the study. BO, SS, and CT: data collection and analysis, and contributions to interpretation of results.

FUNDING

This research has benefited from funding provided by Italian Project PRIN 2017KT2MK.

ACKNOWLEDGMENTS

The authors are grateful to the Editor Claudia Piromallo and the Reviewers Simone Cesca and Gianfranco Vannucci for their suggestions which helped to improve the manuscript.

REFERENCES

Aloisi, M., Bruno, V., Cannavò, F., Ferranti, L., Mattia, M., Monaco, C., et al. (2013). Are the Source Models of the M 7.1 1908 Messina Straits Earthquake Reliable? Insights from a Novel Inversion and a Sensitivity Analysis of Levelling Data. *Geophys. J. Int.* 192 (3), 1025–1041. doi:10.1093/gji/ggs062

Amato, A., and Mele, F. (2008). Performance of the INGV National Seismic Network from 1997 to 2007. *Ann: Geophys-Italy*. 51 (2-3). doi:10.4401/ag-4454

Amoruso, A., Crescentini, L., Neri, G., Orecchio, B., and Scarpa, R. (2006). Spatial Relation between the 1908 Messina Straits Earthquake Slip and Recent Earthquake Distribution. *Geophys. Res. Lett.* 33, 17. doi:10.1029/2006GL027227

Amoruso, A., Crescentini, L., and Scarpa, R. (2002). Source Parameters of the 1908 Messina Straits, Italy, Earthquake from Geodetic and Seismic Data. *J. Geophys. Res.* 107, 4–1. doi:10.1029/2001JB000434

Barreca, G., Gross, F., Scarfì, L., Aloisi, M., Monaco, C., and Krastel, S. (2021). The Strait of Messina: Seismotectonics and the Source of the 1908 Earthquake. *Earth-Science Rev.* 218, 103685. doi:10.1016/j.earscirev.2021.103685

Bonini, L., Bucci, D. D., Toscani, G., Seno, S., and Valensise, G. (2011). Reconciling Deep Seismogenic and Shallow Active Faults through Analogue Modelling: the

Case of the Messina Straits (Southern Italy). *J. Geol. Soc.* 168 (1), 191–199. doi:10.1144/0016-76492010-055

Boschi, E., Pantosti, D., and Valensise, G. (1989). *Modello di sorgente per il terremoto di Messina del 1908 ed evoluzione recente dell'area dello Stretto*. Roma: Atti VIII Convegno GNGTS, 245–258.

Bottari, A., Capuano, P., De Natale, G., Gasparini, P., Neri, G., Pingue, F., et al. (1989). Source Parameters of Earthquakes in the Strait of Messina, Italy, during This century. *Tectonophysics* 166 (1-3), 221–234. doi:10.1016/0040-1951(89)90215-1

Capuano, P., De Natale, G., Gasparini, P., Pingue, F., and Scarpa, R. (1988). A Model for the 1908 Messina Straits (Italy) Earthquake by Inversion of Levelling Data. *Bull. Seism. Soc. Am.* 78 (6), 1930–1947.

Carafa, M. M. C., Valensise, G., and Bird, P. (2017). Assessing the Seismic Coupling of Shallow continental Faults and its Impact on Seismic hazard Estimates: a Case-Study from Italy. *Geophys. J. Int.* 209 (1), ggx002–47. doi:10.1093/gji/ggx002

Convertito, V., and Pino, N. A. (2014). Discriminating Among Distinct Source Models of the 1908 Messina Straits Earthquake by Modelling Intensity Data through Full Wavefield Seismograms. *Geophys. J. Int.* 198 (1), 164–173. doi:10.1093/gji/ggu128

D'Addezio, G., Pantosti, D., Valensise, G., and Cinti, F. (1993). Investigating the Seismic Potential of Hidden and Semi-hidden Faults: the 1908 Messina Staits and the 1980 Irpinia Earthquakes (Southern Italy). *Z.* Geomorphol. *Supp.* 94, 119–135.

D'Amico, S., Orecchio, B., Presti, D., Gervasi, A., Zhu, L., Guerra, I., et al. (2011). Testing the Stability of Moment Tensor Solutions for Small Earthquakes in the Calabro–Peloritan Arc Region (Southern Italy). *Boll. Geof. Teor. Appl.* 52, 283–298. doi:10.4430/bgta0009

D'Amico, S., Orecchio, B., Presti, D., Zhu, L., Herrmann, R. B., and Neri, G. (2010). Broadband Waveform Inversion of Moderate Earthquakes in the Messina Straits, Southern Italy. *Phys. Earth Planet. In.* 179, 97–106. doi:10.1016/j.pepi.2010.01.012

D'Agostino, N., and Selvaggi, G. (2004). Crustal Motion along the Eurasia-Nubia Plate Boundary in the Calabrian Arc and Sicily and Active Extension in the Messina Straits from GPS Measurements. *J.* Geophys. Res.-Sol. Ea. 109 (B11). doi:10.1029/2004JB002998

De Natale, G., and Pino, N. A. (2014). Comment on 'Are the Source Models of the M 7.1 1908 Messina Straits Earthquake Reliable? Insights from a Novel Inversion and Sensitivity Analysis of Levelling Data' by M. Aloisi, V. Bruno, F. Cannavò, L. Ferranti, M. Mattia, C. Monaco and M. Palano. *Geophys. J. Int.* 197 (3), 1399–1402. doi:10.1093/gji/ggu063

De Natale, G., and Pingue, F. (1987). *Inversione di dati geodetici per modelli di faglia a dislocazione variabile. Applicazione al terremoto di Messina del 1908 Atti 6°Conv*. GNGTS.

De Natale, G., and Pingue, F. (1991). A Variable Slip Fault Model for the 1908 Messina Straits (Italy) Earthquake, by Inversion of Levelling Data. *Geophys. J. Int.* 104 (1), 73–84. doi:10.1111/j.1365-246X.1991.tb02494.x

Devoti, R., Riguzzi, F., Cuffaro, M., and Doglioni, C. (2008). New GPS Constraints on the Kinematics of the Apennines Subduction. *Earth Planet. Sci. Lett.* 273, 163–174. doi:10.1016/j.epsl.2008.06.031

DISS Working Group (2018). Database of Individual Seismogenic Sources (DISS), .version 3.2.1: a compilation of potential sources for earthquakes larger thanM 5.5 in Italy and surrounding areas (Rome: Istituto Nazionale di Geofisica e Vulcanologia). Available at: http://diss.rm.ingv.it/diss/

Doglioni, C., Ligi, M., Scrocca, D., Bigi, S., Bortoluzzi, G., Carminati, E., et al. (2012). The Tectonic Puzzle of the Messina Area (Southern Italy): Insights from New Seismic Reflection Data. *Sci. Rep.* 2 (1), 1–9. doi:10.1038/srep00970

Ekström, G., Nettles, M., and Dziewoński, A. M. (2012). The Global CMT Project 2004-2010: Centroid-Moment Tensors for 13,017 Earthquakes. *Phys. Earth Planet. In.* 200, 1–9. doi:10.1016/j.pepi.2012.04.002

Faccenna, C., Davy, P., Brun, J.-P., Funiciello, R., Giardini, D., Mattei, M., et al. (1996). The Dynamics of Back-Arc Extension: an Experimental Approach to the Opening of the Tyrrhenian Sea. *Geophys. J. Int.* 126, 781–795. doi:10.1111/j.1365-246X.1996.tb04702.x

Faccenna, C., Molin, P., Orecchio, B., Olivetti, V., Bellier, O., Funiciello, F., et al. (2011). Topography of the Calabria Subduction Zone (Southern Italy): Clues for the Origin of Mt. Etna. *Tectonics* 30, TC1003. doi:10.1029/2010TC002694

Ferranti, L., Antonioli, F., Anzidei, M., Monaco, C., and Stocchi, P. (2010). The Timescale and Spatial Extent of Vertical Tectonic Motions in Italy: Insights from Relative Sea-Level Changes Studies. *J. Virtual Explorer* 36, 30. doi:10.3809/jvirtex.2009.0025510.3809/jvirtex.2010.00255

Ferranti, L., Monaco, C., Antonioli, F., Maschio, L., Kershaw, S., and Verrubbi, V. (2007). The Contribution of Regional Uplift and Coseismic Slip to the Vertical Crustal Motion in the Messina Straits, Southern Italy: Evidence from Raised Late Holocene Shorelines. *J. Geophys. Res.* 112 (B6). doi:10.1029/2006JB004473

Fu, L., Heidarzadeh, M., Cukur, D., Chiocci, F. L., Ridente, D., Gross, F., et al. (2017). Tsunamigenic Potential of a Newly Discovered Active Fault Zone in the Outer Messina Strait, Southern Italy. *Geophys. Res. Lett.* 44 (5), 2427–2435. doi:10.1002/2017GL072647

Ghisetti, F. (1992). Fault Parameters in the Messina Strait (Southern Italy) and Relations with the Seismogenic Source. *Tectonophysics* 210 (1-2), 117–133. doi:10.1016/0040-1951(92)90131-o

Goswami, R., Mitchell, N. C., Argnani, A., and Brocklehurst, S. H. (2014). Geomorphology of the Western Ionian Sea between Sicily and Calabria, Italy. *Geo-mar. Lett.* 34 (5), 419–433. doi:10.1007/s00367-014-0374-2

Hollenstein, C., Kahle, H.-G., Geiger, A., Jenny, S., Goes, S., and Giardini, D. (2003). New GPS Constraints on the Africa-Eurasia Plate Boundary Zone in Southern Italy. *Geophys. Res. Lett.* 30 (18). doi:10.1029/2003GL017554

Jacques, E., Monaco, C., Tapponnier, P., Tortorici, L., and Winter, T. (2001). Faulting and Earthquake Triggering during the 1783 Calabria Seismic Sequence. *Geophys. J. Int.* 147, 499–516. doi:10.1046/j.0956-540x.2001.01518.x

Loperfido, A. (1909). Livellazione geometrica di precisione eseguita dall'IGM sulla costa orientale della Sicilia, da Messina a Catania, a Gesso ed a Faro Peloro e sulla costa occidentale della Calabria da Gioia Tauro a Melito di Porto Salvo Relazione della Commissione Reale incaricata di designare filezone più adatte per la ricostruzione degli abitati colpiti dal terremoto del 28 dicembre 1908 o da altri precedenti, 131–156.

Malinverno, A., and Ryan, W. B. F. (1986). Extension in the Tyrrhenian Sea and Shortening in the Apennines as Result of Arc Migration Driven by Sinking of the Lithosphere. *Tectonics* 5 (2), 227–245. doi:10.1029/TC005i002p00227

Meschis, M., Roberts, G. P., Mildon, Z. K., Robertson, J., Michetti, A. M., and Faure Walker, J. P. (2019). Slip on a Mapped normal Fault for the 28th December 1908 Messina Earthquake (Mw 7.1) in Italy. *Sci. Rep.* 9 (1), 1–8. doi:10.1038/s41598-019-42915-2

Monaco, C., and Tortorici, L. (2000). Active Faulting in the Calabrian Arc and Eastern Sicily. *J. Geodyn.* 29 (3-5), 407–424. doi:10.1016/S0264-3707(99)00052-6

Monaco, C., Tortorici, L., Nicolich, R., Cernobori, L., and Costa, M. (1996). From Collisional to Rifted Basins: An Example from the Southern Calabrian Arc (Italy). *Tectonophysics* 266 (1/4), 233–249. doi:10.1016/S0040-1951(96)00192-8

Mulargia, F., and Boschi, E. (1983). The 1908 Messina Earthquake and Related Seismicity, *Earthquakes: observation, Theor. interpretation*, 493–518.

Negredo, A. M., Carminati, E., Barba, S., and Sabadini, R. (1999). Dynamic Modelling of Stress Accumulation in central Italy. *Geophys. Res. Lett.* 26, 13, 1945–1948. doi:10.1029/1999GL900408

Neri, G., Marotta, A. M., Orecchio, B., Presti, D., Totaro, C., Barzaghi, R., et al. (2012). How Lithospheric Subduction Changes along the Calabrian Arc in Southern Italy: Geophysical Evidences. *Int. J. Earth Sci. (Geol Rundsch)* 101, 1949-1969. doi:10.1007/s00531-012-0762-7

Neri, G., Orecchio, B., Scolaro, S., and Totaro, C. (2020). Major Earthquakes of Southern Calabria, Italy, into the Regional Geodynamic Context. *Front. Earth Sci.* 8, 579846. doi:10.3389/feart.2020.579846

Neri, G., Orecchio, B., Totaro, C., Falcone, G., and Presti, D. (2009). Subduction beneath Southern Italy Close the Ending: Results from Seismic Tomography. *Seismological Res. Lett.* 80, 63–70. doi:10.1785/gssrl.80.1.63

Nocquet, J.-M. (2012). Present-day Kinematics of the Mediterranean: A Comprehensive Overview of GPS Results. *Tectonophysics* 579, 220–242. doi:10.1016/j.tecto.2012.03.037

Orecchio, B., Presti, D., Totaro, C., D'Amico, S., and Neri, G. (2015). Investigating Slab Edge Kinematics through Seismological Data: The Northern Boundary of the Ionian Subduction System (South Italy). *J. Geodynamics* 88, 23–35. doi:10.1016/j.jog.2015.04.003

Orecchio, B., Presti, D., Totaro, C., and Neri, G. (2014). What Earthquakes Say Concerning Residual Subduction and STEP Dynamics in the Calabrian Arc Region, South Italy. *Geophys. J. Int.* 199 (3), 1929–1942. doi:10.1093/gji/ggu373

Orecchio, B., Scolaro, S., Batlló, J., Ferrari, G., Presti, D., and Stich, D. (2019). A Reappraisal of the 1978 Ferruzzano Earthquake (Southern Italy) from New Estimates of Hypocenter Location and Moment Tensor Inversion. *Phys. Earth Planet. Interiors* 289, 34–44. doi:10.1016/j.pepi.2019.02.003

Palano, M. (2015). On the Present-Day Crustal Stress, Strain-Rate fields and Mantle Anisotropy Pattern of Italy. *Geophys. J. Int.* 200 (2), 969–985. doi:10.1093/gji/ggu451

Pino, N. A., Giardini, D., and Boschi, E. (2000). The December 28, 1908, Messina Straits, Southern Italy, Earthquake: Waveform Modeling of Regional Seismograms. *J. Geophys. Res.* 105 (B11), 25473–25492. doi:10.1029/2000JB900259

Pizzino, L., Burrato, P., Quattrocchi, F., and Valensise, G. (2004). Geochemical Signatures of Large Active Faults: The Example of the 5 February 1783, Calabrian Earthquake (Southern Italy). *J. Seismology* 8, 363–380. doi:10.1023/B:JOSE.0000038455.56343.e7

Polonia, A., Torelli, L., Artoni, A., Carlini, M., Faccenna, C., Ferranti, L., et al. (2016). The Ionian and Alfeo-Etna Fault Zones: New Segments of an Evolving Plate Boundary in the central Mediterranean Sea? *Tectonophysics* 675, 69–90. doi:10.1016/j.tecto.2016.03.016

Pondrelli, S., Salimbeni, S., Ekström, G., Morelli, A., Gasperini, P., and Vannucci, G. (2006). The Italian CMT Dataset from 1977 to the Present. *Phys. Earth Planet. Interiors* 159 (3-4), 286–303. doi:10.1016/j.pepi.2006.07.008

Presti, D., Billi, A., Orecchio, B., Totaro, C., Faccenna, C., and Neri, G. (2013). Earthquake Focal Mechanisms, Seismogenic Stress, and Seismotectonics of the Calabrian Arc, Italy. *Tectonophysics* 602, 153–175. doi:10.1016/j.tecto.2013.01.030

Presti, D., Neri, G., Orecchio, B., Scolaro, S., and Totaro, C. (2017). The 1905 Calabria, Southern Italy, Earthquake: Hypocenter Location, Causative Process, and Stress Changes Induced in the Area of the 1908 Messina Straits Earthquake. *Bull. Seismol. Soc. Am.* 107 (6), 2613–2623. doi:10.1785/0120170094

Presti, D., Orecchio, B., Falcone, G., and Neri, G. (2008). Linear versus Non-linear Earthquake Location and Seismogenic Fault Detection in the Southern Tyrrhenian Sea, Italy. *Italy.* Geophys. J. Int. 172, 607–618. doi:10.1111/j.1365-246X.2007.03642.x

Presti, D. (2019). Seismicity Supports the Theory of Incipient Rifting in the Western Ionian Sea, central Mediterranean. *Ann. Geophys-italy* 62 (2), 225. doi:10.4401/ag-8360

Presti, D., Totaro, C., Neri, G., and Orecchio, B. (2019). New Earthquake Data in the Calabrian Subduction Zone, Italy, Suggest Revision of the Presumed Dynamics in the Upper Part of the Subducting Slab. *Seismol. Res. Lett.* 90 (5), 1994–2004. doi:10.1785/0220190024

Presti, D., Troise, C., and De Natale, G. (2004). Probabilistic Location of Seismic Sequences in Heterogeneous media. *Bull. Seismological Soc. America* 94, 2239–2253. doi:10.1785/0120030160

Ridente, D., Martorelli, E., Bosman, A., and Chiocci, F. L. (2014). High-resolution Morpho-Bathymetric Imaging of the Messina Strait (Southern Italy). New Insights on the 1908 Earthquake and Tsunami. *Geomorphology* 208, 149–159. doi:10.1016/j.geomorph.2013.11.021

Rosenbaum, G., Lister, G. S., and Duboz, C. (2002). Reconstruction of the Tectonic Evolution of the Western Mediterranean since the Oligocene. *J.Virt.Ex* 08 (6). doi:10.3809/jvirtex.2002.00053

Schick, R. (1977). Eine seimotektonische Bearbeitung des Erdbedens von Messina aus dem Jahre 1908. Geol. Jb. *E-* 11, 3–74.

Schorlemmer, D., Mele, F., and Marzocchi, W. (2010). A Completeness Analysis of the National Seismic Network of Italy. *J. Geophys. Res.* 115 (B4). doi:10.1029/2008JB006097

Scolaro, S., Totaro, C., Presti, D., D'Amico, S., Neri, G., and Orecchio, B. (2018). Estimating Stability and Resolution of Waveform Inversion Focal Mechanisms. In *Moment Tensor Solutions*. Springer, 93–109. doi:10.1007/978-3-319-77359-9_5

Selli, R., Colantoni, P., Fabri, A., Rossi, S., and Borsetti, A. M. (1978). Marine Geological Investigations on the Messina Strait and its Approaches. *Giorn. Geol.* 42 (2).

Serpelloni, E., Faccenna, C., Spada, G., Dong, D., and Williams, S. D. P. (2013). Vertical GPS Ground Motion Rates in the Euro-Mediterranean Region: New Evidence of Velocity Gradients at Different Spatial Scales along the Nubia-Eurasia Plate Boundary. *J. Geophys. Res. Solid Earth* 118 (11), 6003–6024. doi:10.1002/2013JB010102

Tiberti, M. M., Vannoli, P., Fracassi, U., Burrato, P., Kastelic, V., and Valensise, G. (2017). Understanding Seismogenic Processes in the Southern Calabrian Arc:A Geodynamic Perspective. *Ijg* 136 (3), 365–388. doi:10.3301/IJG.2016.12

Totaro, C., Orecchio, B., Presti, D., Scolaro, S., and Neri, G. (2016). Seismogenic Stress Field Estimation in the Calabrian Arc Region (South Italy) from a Bayesian Approach. *Geophys. Res. Lett.* 43 (17), 8960–8969. doi:10.1002/2016GL070107

Valensise, G., and D'Addezio, G. (1994). *Il contributo della geologia di superficie all'individuazione delle strutture sismogenetiche della Piana di Gioia Tauro*, Istituto Nazionale di Geofisica internal publication No., 559, 21 pp.

Valensise, G., and Pantosti, D. (1992). A 125 Kyr-Long Geological Record of Seismic Source Repeatability: the Messina Straits (Southern Italy) and the 1908 Earthquake (Ms7/2). *Terra Nova* 4 (4), 472–483. doi:10.1111/j.1365-3121.1992.tb00583.x

Zhao, L. S., and Helmberger, D. V. (1994). Source Estimation from Broadband Regional Seismograms. *Bull. Seismol. Soc. Am.* 84 (1), 91–104.

Zhu, L., and Helmberger, D. (1996). Advancement in Source Estimation Technique Using Broadband Regional Seismograms. *Bull. Seismol. Soc. Am.* 86, 1634–1641.

Conflict of Interest: The authors declare that the research was conducted in the absence of any commercial or financial relationships that could be construed as a potential conflict of interest.